The Journal of Experimental Biology 214, 3688-3697

doi:10.1242/jeb.060301

RESEARCH ARTICLE

An evaluation of muscle maintenance costs during fiber hypertrophy in the lobster *Homarus americanus*: are larger muscle fibers cheaper to maintain?

Ana Gabriela Jimenez[1], Santosh K. Dasika[2], Bruce R. Locke[2] and Stephen T. Kinsey[1,*]

[1]Department of Biology and Marine Biology, University of North Carolina Wilmington, Wilmington, NC 28403, USA and [2]Department of Chemical and Biomedical Engineering, Florida State University, FAMU-FSU, College of Engineering, 2525 Pottsdamer Street, Tallahassee, FL 32310, USA

*Author for correspondence (kinseys@uncw.edu)

Accepted 10 August 2011

SUMMARY

Large muscle fiber size imposes constraints on muscle function while imparting no obvious advantages, making it difficult to explain why muscle fibers are among the largest cell type. Johnston and colleagues proposed the 'optimal fiber size' hypothesis, which states that some fish have large fibers that balance the need for short diffusion distances against metabolic cost savings associated with large fibers. We tested this hypothesis in hypertrophically growing fibers in the lobster *Homarus americanus*. Mean fiber diameter was 316±11 μm in juveniles and 670±26 μm in adults, leading to a surface area to volume ratio (SA:V) that was 2-fold higher in juveniles. Na^+/K^+-ATPase activity was also 2-fold higher in smaller fibers. ^{31}P-NMR was used with metabolic inhibitors to determine the cost of metabolic processes in muscle preparations. The cost of Na^+/K^+-ATPase function was also 2-fold higher in smaller than in larger diameter fibers. Extrapolation of the SA:V dependence of the Na^+/K^+-ATPase over a broad fiber size range showed that if fibers were much smaller than those observed, maintenance of the membrane potential would constitute a large fraction of whole-animal metabolic rate, suggesting that the fibers grow large to reduce maintenance costs. However, a reaction–diffusion model of aerobic metabolism indicated that fibers in adults could attain still larger sizes without diffusion limitation, although further growth would have a negligible effect on cost. Therefore, it appears that decreased fiber SA:V makes larger fibers in *H. americanus* less expensive to maintain, which is consistent with the optimal fiber size hypothesis.

Key words: crustacean, muscle physiology, basal metabolism.

INTRODUCTION

The size of fibers within skeletal muscle is a fundamental property that influences function and reflects the patterns of muscle growth that have occurred throughout an organism's life. It is generally accepted that constraints associated with processes like aerobic metabolism, which relies on oxygen diffusion, limit the maximal fiber size (Van Wessel et al., 2010). However, there is no similar conceptual framework to explain the regulation of minimal fiber size. This gap in understanding is particularly glaring when considering that in adult animals fiber diameter varies across species over 3 orders of magnitude, from a few micrometers to more than 5 mm (e.g. Kinsey et al., 2007). Muscle grows by a combination of hyperplasia, which is an increase in fiber number, and hypertrophy, which is an increase in fiber size. Anaerobic muscle grows primarily by hypertrophy in crustaceans (Bittner and Traut, 1978; Boyle et al., 2003; Jimenez et al., 2008) and fish (Weatherly and Gill, 1985; Valente et al., 1999; Nyack et al., 2007), which when coupled to a dramatic post-metamorphic increase in body mass leads to very large fibers in adults (Kinsey et al., 2007). As anaerobic fibers in these groups grow, there are changes in mitochondrial and nuclear distribution, as well as a shift away from hypertrophic growth once a threshold size is reached, and mathematical reaction–diffusion models indicate that these are responses aimed at offsetting diffusion constraints that would otherwise arise in adult animals (Fine et al., 1993; Boyle et al., 2003; Nyack et al., 2007; Hardy et al., 2009; Hardy et al., 2010; Kinsey et al., 2011; Priester et al., 2011).

Because large fiber size appears to impose constraints on muscle function, it has been difficult to explain why selection might favor large fibers. Johnston and colleagues (Johnston et al., 2003; Johnston et al., 2004; Johnston et al., 2006) proposed the 'optimal fiber size hypothesis' to explain the very large fibers observed in the white muscle of some fish. These authors proposed that fish may balance the need for small fibers that promote rapid diffusive flux against potential metabolic cost savings associated with large fibers. Specifically, the fiber surface area over which membrane potential must be maintained is reduced as fibers grow, presumably making large fibers cheaper to maintain.

The major components of basal ATP consumption in mammalian muscle are the active transport of Na^+ and K^+ across the sarcolemmal membrane by the Na^+/K^+-ATPase, Ca^{2+} transport across the sarcoplasmic reticulum (SR) membrane by the SR Ca^{2+}-ATPase, and protein turnover, which consumes one GTP molecule for every amino acid translated (Gregg and Milligan, 1982; Rolfe and Brand, 1996). The Na^+/K^+-ATPase functions to maintain the membrane potential across the sarcolemma, pumping three Na^+ ions out of the cell and two K^+ ions into the cell for every ATP hydrolyzed (Milligan and McBride, 1985). The SR is the largest Ca^{2+}-storing compartment in any tissue (Clausen et al., 1991), and the SR Ca^{2+}-ATPase is the major mechanism for Ca^{2+} sequestration in the SR in active and resting muscle (Milligan and McBride, 1985; Swaminathan et al., 1989; Clausen et al., 1991; Györke and Palade, 1992). Lastly, protein turnover in mammalian skeletal muscle entails transcription and translation, as

well as processes associated with protein degradation, and it can represent more than 25% of total basal metabolic rate in mammalian muscle (Gill et al., 1989; Rolfe and Brown, 1997). Of these three processes, only the cost of the Na^+/K^+-ATPase would be expected to be dependent on fiber size, where the decrease in fiber surface area to volume ratio (SA:V) that occurs as fibers grow larger may lead to reduced costs associated with maintaining the membrane potential (Johnston et al., 2003; Johnston et al., 2004; Johnston et al., 2006).

While skeletal muscle is generally thought to have a low resting metabolic rate compared with other tissues, it often makes up a large fraction of body mass. In humans, skeletal muscle comprises about 40% of body mass in healthy adult subjects and 20–30% of the total resting O_2 uptake is devoted to maintaining muscle mass (Zurlo et al., 1990). In fish and crustaceans, muscle can make up a much larger fraction of total body mass and therefore may be under strong selection to have low maintenance costs. For example, in tail-flipping crustaceans, abdominal musculature may comprise up to 65% of the total body mass of the animal (Jimenez et al., 2008) and in fish, muscle makes up 30–80% of body mass (Weatherley and Gill, 1987). As ionic homeostasis comprises 20–40% of the resting metabolic rate in fish (Jobling, 1994), and muscle is the dominant tissue in terms of mass in fish and crustaceans, large fibers may promote a sizable energetic saving in these animals.

In the current study, we specifically tested whether Na^+–K^+ pumping is proportional to fiber SA:V, and whether larger fibers are cheaper to maintain as a result of a lower SA:V. We examined this in anaerobic (white) fibers from abdominal muscle of two size classes (juveniles and adults) of the American lobster, *Homarus americanus*. Because of hypertrophic growth, juvenile animals have relatively small fibers while adults have relatively large fibers, providing a means of testing this hypothesis in a single species. Abdominal muscle makes up a substantial fraction of this animal's body mass, but it is used only occasionally to power a tail-flipping escape response. There might, therefore, be strong selective pressure to minimize maintenance costs of this large, but infrequently used, muscle mass, and the abdominal musculature in adults is, in fact, known to be composed of large fibers. We applied a reaction–diffusion model to address whether fibers from adult animals are near an optimal size that minimizes costs while avoiding diffusion limitation, which would be consistent with the optimal fiber size hypothesis proposed by Johnston and colleagues (Johnston et al., 2003; Johnston et al., 2004; Johnston et al., 2006).

MATERIALS AND METHODS

Animal care and maintenance

Adult lobsters (*Homarus americanus*, H. Milne-Edwards 1837) were caught in Maine, and then shipped to vendors in Wilmington, NC, where they were maintained in holding tanks at 10°C prior to purchase. Juvenile lobsters were obtained by the Massachusetts Division of Marine Fisheries and then shipped to the University of North Carolina Wilmington. Juvenile and adult size classes were largely dictated by the size ranges that were available, but the two size classes did not overlap in body length or body mass (see Results for details). All animals were maintained in tanks containing filtered seawater that was constantly aerated, at a temperature of 10–12°C and a photoperiod of 12 h:12 h L:D for at least 24 h prior to experimentation. Temperature was monitored daily using a Barnant 115 thermocouple thermometer (Cole-Parmer, Vernon Hills, IL, USA), and water quality (nitrates, nitrites, pH and ammonia) was monitored weekly using a Salt Water Master Kit (Aquarium Pharmaceuticals, Chalfont, PA, USA). Animals were fed every other day; however, feeding was stopped 24 h prior to the start of the experiments.

Fiber diameter measurements

Fiber diameter was measured to confirm that the juvenile size class had smaller fibers than the adult size class as a result of hypertrophic growth. Lobsters were injected in the dorsal vein sinus with a 250 μg ml^{-1} solution of wheat germ agglutinin (WGA) labeled with Alexa Fluor 488. WGA is a lectin that binds to glycoproteins on the basement membrane of the fiber sarcolemma (Wright, 1984) and effectively outlines the fiber periphery to allow measurement of fiber size (Jimenez et al., 2008; Jimenez et al., 2010; Hardy et al., 2009). Animals were provoked to tail flip after the injection to promote perfusion of the stain into muscle fibers. Animals were killed by rapidly severing the abdomen and cephalothorax, and abdominal extensor muscle was excised 30 min after injection, flash frozen in isopentane cooled in liquid nitrogen, and then mounted at resting length in optimal cutting temperature (OCT) compound (Sakura Finetek, Torrence, CA, USA) and allowed to equilibrate to –19°C in a Reichert–Jung/Leica 1800 cryocut microtome (Depew, NY, USA) before sectioning. Sections were cut at 30 μm, picked up on slides, air-dried at room temperature and then mounted. Stained slides were examined with an Olympus Fluoview 1000 laser scanning confocal microscope (Center Valley, PA, USA) and images were recorded as 1 μm thick optical sections. Polygons were traced along the fiber periphery using Adobe Photoshop (version 7.0) and Image Pro Plus (version 6.0) was used to analyze fiber diameter. The average diameter of the polygon traces through the centroid was calculated in 2 deg increments around the circumference of the cell (Nyack et al., 2007; Jimenez et al., 2008; Jimenez et al., 2010).

Cost of metabolic processes

We examined the energetics of anaerobic muscle tissue from juvenile and adult *H. americanus* using *ex vivo* ^{31}P-NMR techniques on small fiber preparations. Abdominal muscle tissue was dissected, and bundles of several fibers (1–2 mm diameter) were tied at resting length to a section of rigid tubing and placed in oxygenated lobster saline (452 mmol l^{-1} NaCl, 15 mmol l^{-1} KCl, 18.9 mmol l^{-1} $CaCl_2$, 4 mmol l^{-1} $MgCl_2$, 2.8 mmol l^{-1} $MgSO_4$ equilibrated with 99.5% O_2/0.5% CO_2, pH 7.4) for 15 min to stabilize. Immediately before the experiments began, the tubing with the muscle was placed in a 5 mm NMR tube containing non-oxygenated saline and one of four treatments (see below). The cost of metabolic processes was determined by monitoring the rate of decrease of arginine phosphate (AP) in the presence of various metabolic inhibitors. AP is in equilibrium with ATP, ADP and arginine because of the high activity of arginine kinase (AK) in crustacean anaerobic muscle. Thus, when the metabolic production of ATP is inhibited, the rate of AP depletion is equivalent to the rate of ATP demand. Muscle basal metabolic rate was measured by monitoring the rate of AP decrease in the presence of 2.5 mmol l^{-1} potassium cyanide to block oxidative phosphorylation and 1 mmol l^{-1} sodium iodoacetate to block glycolysis in lobster saline. The cost of the Na^+/K^+-ATPase, SR Ca^{2+}-ATPase and transcription+translation was determined from the reduction in the rate of AP depletion when energy metabolism was blocked as above, while simultaneously inhibiting these processes with 5 mmol l^{-1} ouabain, 10 mmol l^{-1} nifidipine plus 10 mmol l^{-1} thapsigargin, or 20 μg ml^{-1} actinomycin D plus 200 μg ml^{-1} puromycin, respectively.

NMR spectra were collected at 162 MHz on a Bruker 400 DMX spectrometer (Billerica, MA, USA) to determine relative

concentrations of AP, ATP and inorganic phosphate (P_i). Spectra were collected every 3 min using a 90 deg excitation pulse and a relaxation delay of 12 s, which ensured that the phosphorus nuclei were fully relaxed and peak integrals for the metabolites were proportional to their relative concentrations. The area under each peak was integrated using TopSpin-NMR software (Bruker) to yield relative concentrations of each metabolite, and these values were converted to concentration by assuming a total high-energy phosphate (HEP) concentration of 50 mmol l^{-1}, which is characteristic of crustacean white muscle (Kinsey et al., 2005).

To ensure that glycolysis was blocked during these experiments, lactate concentration was measured spectrophotometrically. Muscle lactate was measured after dissected muscle fibers from adult *H. americanus* were subjected to conditions identical to those in some of the ^{31}P-NMR experiments. The treatments used were as follows: muscles were incubated for 110 min in oxygenated lobster saline, incubated with 2.5 mmol l^{-1} potassium cyanide and 1 mmol l^{-1} sodium iodoacetate with no oxygenation for 15 min and 110 min, and also incubated in 2.5 mmol l^{-1} potassium cyanide, 1 mmol l^{-1} sodium iodoacetate and 5 mmol l^{-1} ouabain with no oxygenation for 15 min and 110 min. These experiments allowed us to evaluate lactate content at time points comparable to the beginning (15 min) and end (110 min) of the NMR experiments. Frozen tissue samples and the surrounding saline solution were homogenized in 3- to 10-fold dilutions of chilled 7% (v/v) perchloric acid with 1 mmol l^{-1} EDTA, and then centrifuged at 4°C at 16,000 ***g*** for 30 min. The supernatant was neutralized using 3 mol l^{-1} potassium bicarbonate in 50 mmol l^{-1} PIPES and centrifuged at 4°C at 16,000 ***g*** for 15 min. The resulting supernatant was stored at –80°C until use. The concentration of L-lactate in the extract was spectrophotometrically assayed following the procedures of Lowry and Passonneau (Lowry and Passonneau, 1972) [as modified by Kinsey and Ellington (Kinsey and Ellington, 1996)]. A buffer containing 300 mmol l^{-1} hydrazine hydrate, 12 mmol l^{-1} EDTA and 4 mmol l^{-1} NAD^+ at pH 9.0 was mixed with the tissue extract in a 0.5 ml cuvette and absorbance was monitored at a wavelength of 340 nm on a Pharmacia Ultrospec 4000 spectrophotometer (Pfizer, New York, NY, USA) to obtain a stable baseline. The reaction was initiated by the addition of 18.5 U of L-lactate dehydrogenase, and the change in absorbance was measured.

Maximal activity of the Na^+/K^+-ATPase

Na^+/K^+-ATPase activity was assayed to provide a measure of the fiber size dependence of the capacity for Na^+ and K^+ transport in order to compare this with the measurements of cost described above. A K^+-stimulated 3-*O*-methylfluorescein phosphatase (MFPase) assay was used to measure the maximal activity of the Na^+/K^+-ATPase (Fraser and McKenna, 1998; Barr et al., 2005; Sandiford et al., 2005). Muscle tissue was dissected, frozen in liquid nitrogen, and homogenized at 0–4°C for 2×20 s at 25,000 r.p.m. with a Fisher Powergen 125 homogenizer (Pittsburgh, PA, USA) in 250 mmol l^{-1} sucrose, 2 mmol l^{-1} EDTA, 1.25 mmol l^{-1} EGTA, 5 mmol l^{-1} NaN_3 and 10 mmol l^{-1} Tris (pH 7.4). Homogenates were freeze-thawed 4 times to break up vesicles and fully expose the binding sites, diluted 1:5 in cold homogenate buffer and then further incubated in a buffer containing 5 mmol l^{-1} $MgCl_2$, 1.25 mmol l^{-1} EDTA, 100 mmol l^{-1} Tris base (pH 7.4), 1 mmol l^{-1} EGTA and 5 mmol l^{-1} NaN_3. Activity was determined using spectrofluorometry at an excitation wavelength of 475 nm and an emission wavelength of 515 nm (Promega Luminometer 20/20 with a Glomax blue module; Madison, WI, USA). The addition of 160 μmol l^{-1} 3-*O*-methylfluorescein phosphate initiated the reaction and the linear increase in fluorescence was recorded, followed by an addition of 10 μmol l^{-1} KCl. K^+-dependent 3-*O*-MFPase activity was determined by subtracting activity before the addition of KCl from activity after the addition of KCl.

Na^+/K^+-ATPase localization

Large crustacean muscle fibers have sarcolemmal invaginations called clefts that are part of the T-tubule system (Peachy, 1967; Selverston, 1967; Rossner and Sherman, 1978). To confirm that the bulk of the Na^+/K^+-ATPase was located in the sarcolemmal membrane, rather than in clefts or in other intracellular locations, an immunohistochemical protocol was used based on the method of Barradas and colleagues (Barradas et al., 1999). Animals were killed by rapidly severing the abdomen and cephalothorax, and abdominal extensor muscle was excised tissues were dissected and fixed in 4% (v/v) paraformaldehyde for 4 h at room temperature, and tissues were mounted in OCT and sectioned as described above. Sections were blocked with a 5% (v/v) normal goat serum (NGS) in a PBS buffer containing 0.05% (v/v) Tween 20 and 0.1% (v/v) BSA for 20 min at room temperature. Sections were incubated with a primary antibody (α5 antibody, mouse anti-chicken IgG, obtained from the Developmental Studies Hybridoma Bank) diluted 1:100 in a 1% (v/v) NGS buffer containing 0.05% (v/v) Tween 20 for 75 min in a wet chamber at 37°C. After 3×10 min washes with PBS and 0.05% (v/v) Tween 20 buffer, the sections were incubated with anti-mouse IgG biotin (1:100, Sigma, St Louis, MO, USA) for 1 h at 37°C. Sections were once again washed 3×10 min in a PBS and 0.05% (v/v) Tween 20 buffer. Then, sections were incubated for 30 min with Alexa Fluor 594–avidin conjugate (1:200, Invitrogen, Carlsbad, CA, USA) at room temperature. Following staining procedures, sections were rinsed 3×10 min in PBS and 0.05% (v/v) Tween 20, and rinsed once in PBS. Sections were mounted and images were obtained and processed using an Olympus Fluoview 1000 confocal microscope.

Maximal activity of the SR Ca^{2+}-ATPase

SR Ca^{2+}-ATPase activity was measured to provide an index of fiber size-specific changes in the capacity for Ca^{2+} transport that could be compared with the measured cost of Ca^{2+} transport described above. Activity was determined spectrophotometrically following the protocol of Simonides and van Hardeveld (Simonides and van Hardeveld, 1990) (modified from Carroll et al., 1999; Inashima et al., 2003). Frozen abdominal muscle tissues were pulverized under liquid nitrogen using a mortar and pestle. An aliquot of muscle powder was diluted 1:8 in homogenization buffer (20 mmol l^{-1} Tris HCl, 300 mmol l^{-1} sucrose, 0.2 mmol l^{-1} phenylmethylsulfonyl fluoride) and then homogenized on ice 3 times for 30 s each. A 20 μl aliquot of the homogenate was added to 1 ml of the assay mixture (1 mmol l^{-1} EDTA, 20 mmol l^{-1} Hepes, 200 mmol l^{-1} KCl, 15 mmol l^{-1} $MgCl_2$, 10 mmol l^{-1} NaN_3, 2 mmol l^{-1} EGTA, 10 mmol l^{-1} phosphoenol pyruvate, 0.8 mmol l^{-1} $CaCl_2$, 18 U ml^{-1} pyruvate kinase, 18 U ml^{-1} lactate dehydrogenase, 0.4 mmol l^{-1} NADH and 0.005% (v/v) Triton X-100, with 1 μg per 1 ml of assay of Ca^{2+} ionophore, pH 7.5). The assay was initiated by adding 4 mmol l^{-1} (final concentration) ATP and measured at a wavelength of 340 nm. Finally, the $CaCl_2$ concentration was increased to 20 mmol l^{-1}, which immediately inhibited the SR Ca^{2+}-ATPase. The remaining activity was defined as the background ATPase activity. The activity of SR Ca^{2+}-ATPase was calculated as the difference between total ATPase and the background ATPase activities.

Nuclear number density

Nuclear number density was measured as a proxy for the capacity for transcription and translation, so that fiber size-specific changes in capacity could be compared with the cost of these processes as described above. Muscle tissue was injected with WGA, removed and sectioned as described above. Nuclei were stained with 0.5 μg ml^{-1} DAPI for 30 min. Slides were then rinsed in PBS for 10 min. Optical slices of WGA-injected and DAPI-labeled muscle cross-sections and longitudinal sections were collected with an Olympus Fluoview 1000 confocal microscope. Peripheral muscle nuclei or subsarcolemmal nuclei (SS) were sometimes difficult to distinguish from extracellular nuclei or from nuclei in adjoining fibers. Thus, differential interference contrast images (DIC) and nuclear shape helped us to determine whether peripherally located nuclei were truly intracellular (Hardy et al., 2009; Hardy et al., 2010; Priester et al., 2011). Fiber margins were traced using Adobe Photoshop and resultant polygons were used in Image Pro Plus to calculate fiber cross-sectional area (CSA), while nuclear CSA and diameter (from fiber cross-sections) and nuclear lengths (from longitudinal sections) were calculated by outlining DAPI-stained nuclei. The nuclear number density, which is the number of nuclei per volume of fiber, is the inverse of the nuclear domain and was calculated following the methods of Schmalbruch and Hellhammer (Schmalbruch and Hellhammer, 1977):

$$\text{Nuclear number density} = \frac{N}{(d+l)\times \text{CSA}} \quad , \qquad (1)$$

where N represents the number of myonuclei per cross-section of fiber, d is the thickness of the section (30 μm) and l is the mean length of a muscle nucleus.

Mitochondrial volume density

To estimate aerobic capacity of abdominal extensor muscle for our reaction–diffusion model of aerobic metabolism, mitochondrial volume density was measured using a transmission electron microscope (TEM) following the methods of Nyack et al. (Nyack et al., 2007). Excised abdominal muscle fibers from juvenile and adult lobsters were fixed at room temperature in 2.5% (v/v) glutaraldehyde with 0.2 mol l^{-1} sodium cacodylate buffer for 24 h, rinsed twice for 15 min each in cacodylate buffer and then placed in secondary fixative of OsO_4 for 2 h. Embedding and systematic random thin-sectioning methods followed those described previously (Boyle et al., 2003; Johnson et al., 2004). Sections were examined on a CM-12 TEM (Philips Research, Briarcliff Manor, NY, USA), and micrographs were analyzed by a systematic random sampling method for each grid (Howard and Reed, 1998) as described elsewhere (Nyack et al., 2007; Burpee et al., 2010). Micrographs were then developed and digitized using a Microtek Scanmaker 4 (Microtek Lab, Carson, CA, USA). Four animals of each size class were examined. Three micrographs were collected per grid, giving a total of 15 micrographs per tissue preparation.

Analysis and modeling

The optimal fiber size hypothesis states that fibers are as large as they can be to reduce metabolic costs, without becoming so large that aerobic metabolism is limited by diffusion. To evaluate the relationship between cost of the Na^+/K^+-ATPase and fiber SA:V, a curve that describes the SA:V of a cylindrical fiber as a function of fiber radius was iteratively fitted to the experimental data. This allowed us to project the Na^+/K^+-ATPase costs to smaller and larger fibers than those that were measured and therefore estimate the changing cost during fiber growth.

An existing reaction–diffusion mathematical model was applied to lobster fibers to assess the extent to which diffusion constrains aerobic ATP turnover and therefore limits maximal fiber size (Dasika et al., 2011). The model assumes that O_2 is supplied *via* the hemolymph at the fiber periphery, and that mitochondria, cellular ATPases and AK are distributed uniformly across the radius of the fiber. ATP production at the mitochondria is governed by an expression derived from the detailed model of oxidative phosphorylation developed by Beard (Beard, 2005). This expression serves as a boundary condition where the rate of ATP production is dependent on the concentrations of O_2, ADP and P_i. ATP consumption is governed by a Michaelis–Menten expression with dependence on ATP concentration, and AK was described using the expression of Smith and Morrison (Smith and Morrison, 1969). The effectiveness factor (η) was calculated to quantify the extent to which diffusion limits aerobic ATP turnover. The η is the ratio of the metabolic rate in the presence of diffusion to the rate if diffusion were infinitely fast. Thus, if η=1, then diffusion does not limit the reaction rate, whereas if η=0.5, then the rate is 50% of what it would be if diffusion was not constraining the reaction. This model allowed us to evaluate how diffusion limitations change during fiber growth (for details, see Dasika et al., 2011).

Statistics

The AP depletion rate for each treatment was analyzed using linear regression analysis. Student's *t*-tests were used to compare fiber diameter, SA:V, Na^+/K^+-ATPase maximal activity, SR Ca^{2+}-ATPase maximal activity and nuclear domain differences between size classes. Two-way analysis of variance (ANOVA) was used to test for an interaction between inhibitor treatment (blocking ATP production *versus* blocking ATP production plus one of the three ATP-consuming processes that were measured) and size class on AP depletion rate. One-way ANOVA was used to test for treatment effects on lactate concentration. The results were considered significant if $P<0.05$. Data are presented as means ± s.e.m.

RESULTS

Body mass and fiber size measurements

The current study examined *H. americanus* ranging in body mass from 10.2 to 927.2 g with mean body masses for the juvenile and adult size classes of 108.1±1.89 and 621.7±2.45 g, respectively. Fig. 1 illustrates hypertrophic growth exhibited by the white abdominal extensor muscles leading to larger fiber sizes in adults. Fiber diameter in juvenile animals ranged from 151 to 621 μm, and in adult animals from 356 to 1048 μm. Mean fiber diameter was 316±11 μm in juveniles (N=3) and 670±26 μm in adults (N=5); thus, adult animals had a mean fiber diameter that was about 2-fold greater than that of juvenile animals, and fiber SA:V (calculated assuming that the average fiber was cylindrical) was therefore about 2-fold lower in adult animals. Student's *t*-test indicated that mean fiber sizes (and SA:V) of juvenile and adult size classes were significantly different (Fig. 1 inset).

Measuring the cost of metabolic processes using ^{31}P-NMR

Isolated abdominal muscle fibers from juvenile and adult *H. americanus* displayed good metabolic stability. When tissues were maintained in oxygenated saline, there was no change in AP concentration over the 110 min time course of the experiments. In contrast, addition of inhibitors of glycolysis and oxidative phosphorylation produced linear reductions in AP over time (and corresponding increases in P_i), the rate of which was equivalent to the rate of ATP demand. When other inhibitors were simultaneously

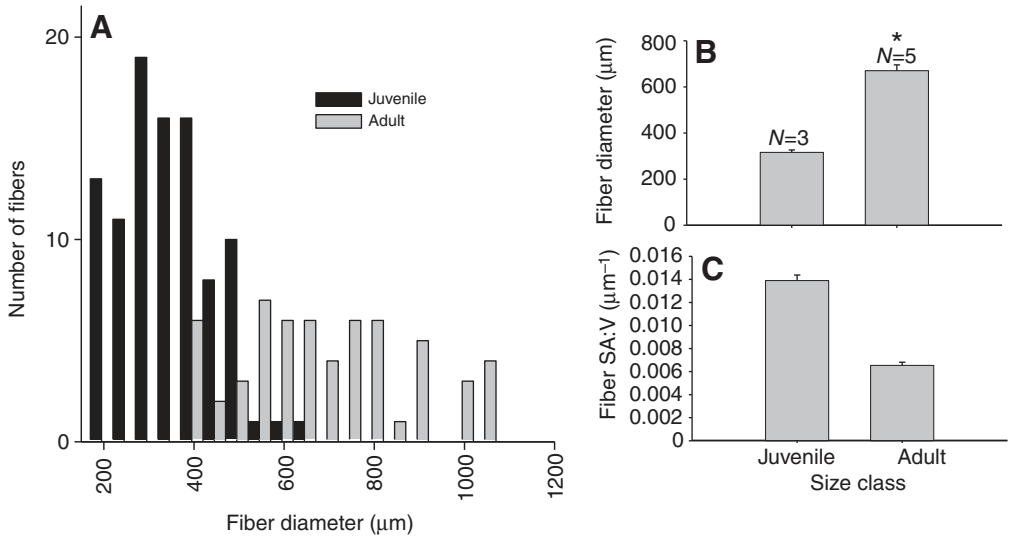

Fig. 1. (A) Abdominal white muscle fiber diameter cross-sectional distribution, (B) mean diameter and (C) surface area to volume ratio (SA:V) from juvenile and adult size classes of *H. americanus*. Asterisk indicates values that are significantly different between size classes. Values are means + s.e.m. and *N* represents the number of animals (96 and 60 fibers were measured in the small and large size class, respectively).

added that blocked specific components of ATP demand, the rate of AP depletion was reduced (Figs 2 and 3). L-Lactate was not higher with inhibitor treatments than in oxygenated saline, and there was no significant effect of treatment on L-lactate concentration, indicating that it did not significantly accumulate during the course of the experiments (F=0.67, P=0.58, N=9 for each treatment).

Fig. 4A shows that the mean AP depletion rate in the presence of inhibitors that blocked ATP production was higher in the small fibers of juveniles than in the large fibers of adults, as expected because of body mass-specific scaling of metabolic rate. In the presence of additional inhibitors that blocked components of ATP demand, the mean rate of AP depletion was reduced. Fig. 4B shows the muscle basal metabolic rate, which is equivalent to the AP depletion rate when ATP production was blocked, as well as the cost of each ATP-consuming component, which is equivalent to the reduction in slope in the presence of an additional inhibitor. Two-way ANOVA revealed a significant interaction of size class and inhibitor treatment on the rate of AP depletion when the Na^+/K^+-ATPase was inhibited (F=7.2472, P=0.0149), whereas there was no significant interaction of size class and treatment on AP depletion rate when Ca^{2+} cycling or transcription+translation was inhibited (the other treatment in all cases was inhibition of ATP production only). This indicates that Na^+/K^+-ATPase cost was fiber size dependent, but Ca^{2+} cycling and transcription+translation cost was not, as hypothesized. Fig. 4B also shows that the basal metabolic rate was largely accounted for by the three processes examined. Further, the Na^+/K^+-ATPase cost was 2-fold higher in smaller fibers of juveniles (consistent with the 2-fold higher SA:V seen in Fig. 1), while there are less dramatic differences in the cost of Ca^{2+} cycling and protein turnover.

Metabolic capacity

Maximal Na^+/K^+-ATPase activity was 2-fold greater in the muscle of juvenile animals than in that of the adult animals, again in proportion to the fiber SA:V (Fig. 5A). There was no significant change in maximal SR Ca^{2+}-ATPase activity between size classes (Fig. 5B), which was consistent with the cost of Ca^{2+} pumping. Total nuclear number volume was significantly greater in the muscle from juveniles than in muscle from adults (Fig. 5C), which was consistent with the difference in cost of transcription and translation. Fig. 5D reveals that, for all cases, the relative changes during growth in metabolic costs were similar to the changes in metabolic capacity of each process. Immunohistochemistry revealed that the Na^+/K^+-ATPase was only detectable at the sarcolemma and no staining was observed in sarcolemmal clefts or in the interior of the fiber, suggesting that most of the activity of this enzyme was localized to the fiber periphery (Fig. 6A). Fig. 6B is a representative image showing stained nuclei

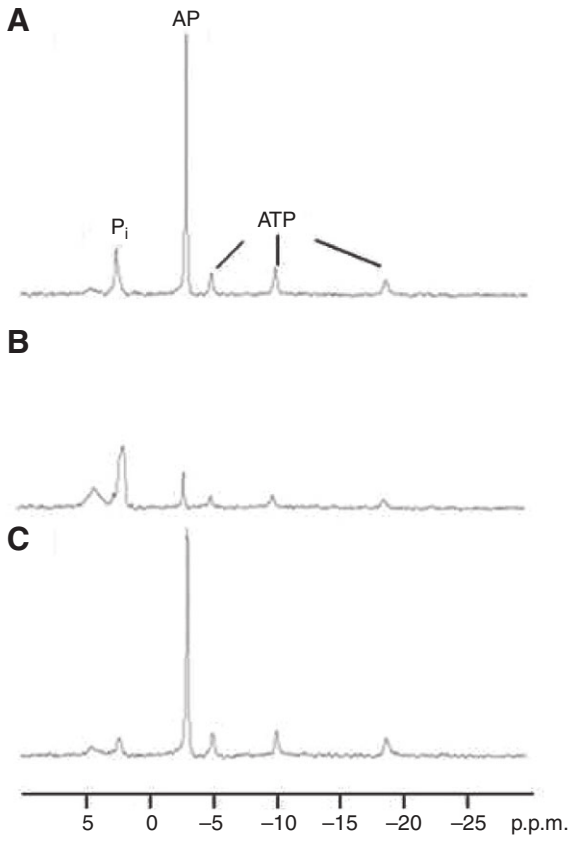

Fig. 2. Example of ^{31}P-NMR spectra. (A) Initial spectrum from an adult lobster in the treatment containing 2.5 mmol l^{-1} potassium cyanide and 1 mmol l^{-1} sodium iodoacetate. (B) Final spectrum after 110 min in the presence of 2.5 mmol l^{-1} potassium cyanide and 1 mmol l^{-1} sodium iodoacetate. (C) Spectrum after 110 min in oxygenated saline in the absence of inhibitors. AP, arginine phosphate; P_i, inorganic phosphate.

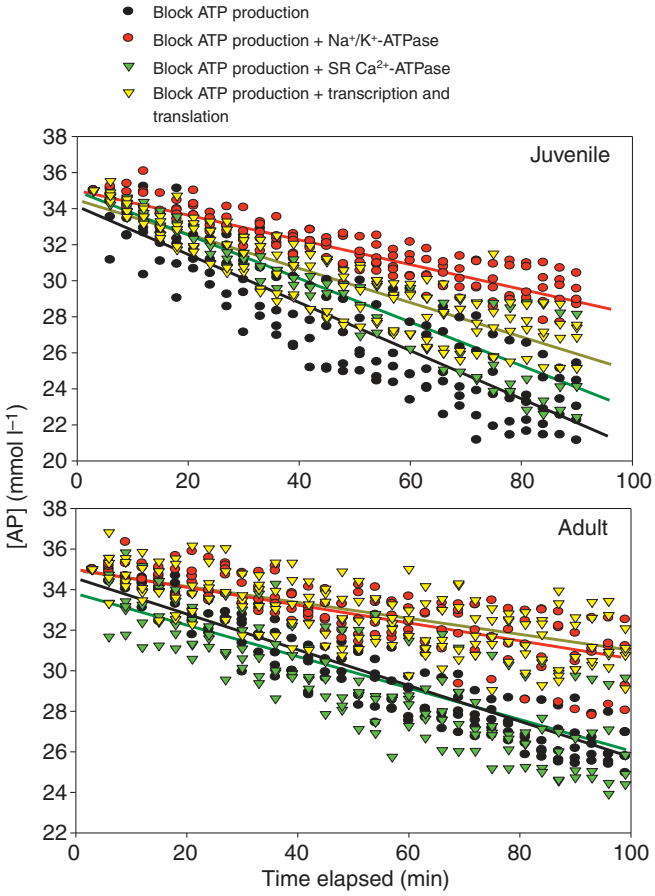

Fig. 3. The rate of AP depletion for the juvenile (top) and adult (bottom) size classes used to measure metabolic costs. Linear regressions for all data in each of the four treatments (pooled for each treatment) are provided for visualization purposes only, but for data analysis a linear regression was applied to each replicate within an experimental treatment (N=5 replicates for each treatment, except for the case where transcription+translation was blocked in the juvenile size class, as only 3 juveniles could be obtained for this treatment). Regression equations for juvenile and adult animals, respectively, were: y=–0.13x+34.26 (r^2=0.79) and y=–0.09x+34.64 (r^2=0.88) when ATP production alone was blocked; y=–0.07x+35.04 (r^2=0.85) and y=–0.04x+34.98 (r^2=0.64) when the Na^+/K^+-ATPase was blocked; y=–0.009x+34.50 (r^2=0.79) and y=–0.04+34.99 (r^2=0.59) when the sarcoplasmic reticulum (SR) Ca^{2+}-ATPase was blocked; and y=–0.012x+34.95 (r^2=0.84) and y=–0.08x+33.82 (r^2=0.70) when transcription+translation was blocked. All regression slopes were significantly different from zero (P<0.05).

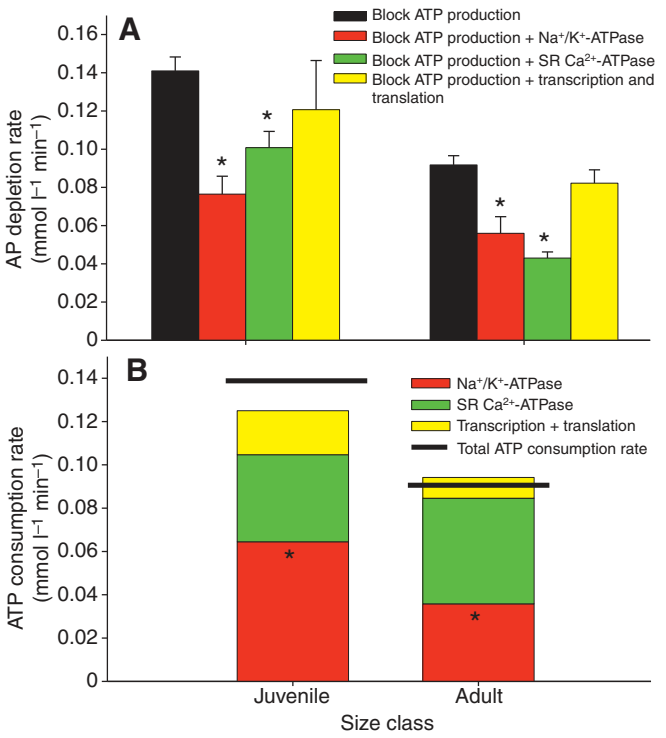

Fig. 4. (A) Mean AP depletion rate for each treatment in juvenile and adult size classes. Asterisks indicate that rates of AP depletion when the Na^+/K^+-ATPase and SR Ca^{2+}-ATPase were inhibited were significantly reduced from the case when ATP production alone was inhibited (Student's t-test, P<0.05). Values are means + s.e.m. (B) Amount of ATP consumed per minute for each process, derived by subtracting the cost when both ATP production and a component of ATP demand were inhibited from the cost when ATP production alone was inhibited. Asterisks indicate that two-way ANOVA detected a significant interaction of size class and inhibitor treatment only for the case when the Na^+/K^+-ATPase was inhibited (P<0.05).

that was used to determine nuclear number density. Nuclei at both the fiber periphery and in the fiber core are common in crustaceans (Jimenez et al., 2010; Hardy et al., 2009; Hardy et al., 2010).

Balancing maintenance costs and diffusion constraints

Fig. 7 shows the predicted decrease in Na^+/K^+-ATPase costs associated with fiber growth, as well as the predicted increase in diffusion limitation of aerobic metabolism as fiber diameter increases. Three different ATP turnover rates are shown in the model results, where the higher rates are associated with a decreased η (and increased diffusion limitation). The maximal ATP turnover rate in lobster abdominal muscle has, to our knowledge, not been measured. However, total mitochondrial volume density was 0.0074±0.0001 for juvenile lobsters and 0.0067±0.0001 for adult lobsters. These volume densities are similar to those in white muscle from other crustaceans for which we have measured rates of aerobic ATP production (Kinsey et al., 2005; Jimenez et al., 2008). Based on this prior work, we believe that a maximal aerobic rate of cellular ATPases ($\dot{V}_{max}$) of 1.2 mmol l^{-1} ATP min^{-1} is the most reasonable rate for lobster abdominal fibers. At this $\dot{V}_{max}$, the fibers do not appear to be approaching substantial diffusion limitation over the fiber size range that is likely to occur.

DISCUSSION

The current study tested whether the cost of maintaining the abdominal muscle of the lobster *H. americanus* decreased during fiber growth. The major findings were that fiber size increased dramatically during animal growth, and SA:V, Na^+/K^+-ATPase activity and the cost of maintaining the membrane potential were 2-fold higher in the smaller fibers of juveniles than in the larger fibers of adults. In contrast, SR Ca^{2+}-ATPase activity and the cost of calcium pumping were independent of fiber size and not significantly different between size classes, while nuclear number density and the cost of transcription and translation were greater in smaller fibers. Therefore, it appears that a decrease in SA:V makes larger muscle fibers metabolically less expensive to maintain, perhaps explaining why muscle fibers are among the largest cells in the animal kingdom.

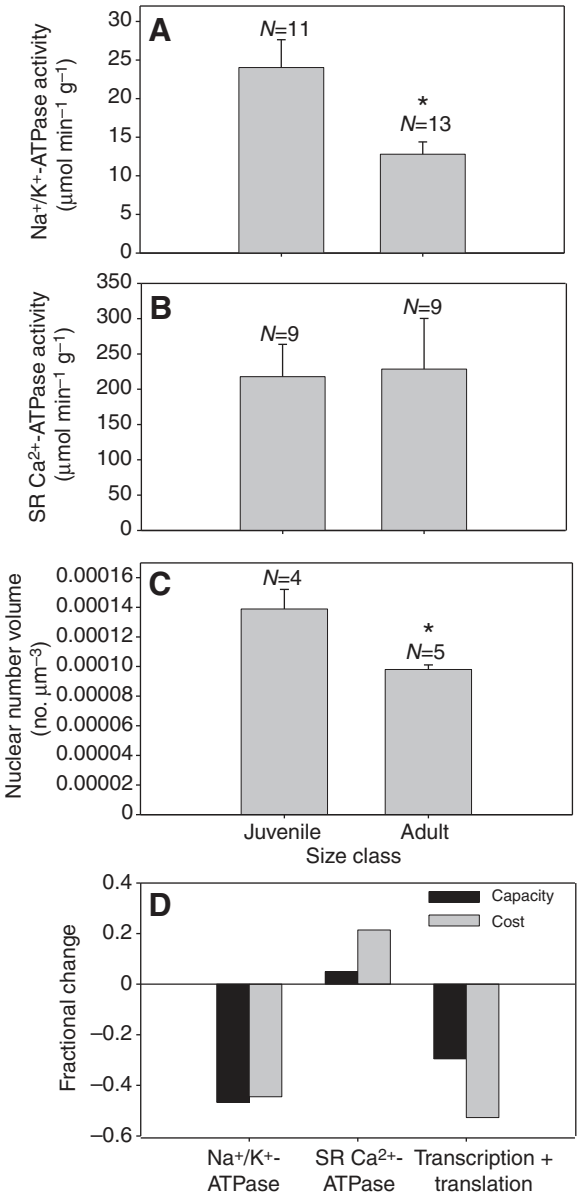

Fig. 5. Metabolic capacity and comparison to metabolic cost in anaerobic fibers of juvenile and adult size classes. (A) Maximal Na^+/K^+-ATPase activity. (B) Maximal SR Ca^{2+}-ATPase activity. (C) Nuclear number density. (D) Fractional change in measurements of capacity and cost during growth from the juvenile to adult animals reveals that the changes in cost are related to changes in capacity. In A and C, the asterisks indicate significant differences between size classes (Student's *t*-test, $P<0.05$). Values are means + s.e.m. and *N* indicates the number of individuals.

Hypertrophic growth leads to developmental increases in diffusion distances that limit the permissible rates of intracellular aerobic processes (Kinsey et al., 2007; Kinsey et al., 2011). In anaerobic fibers like those in the present study, these increased diffusion distances are unlikely to influence contraction, which is powered by phosphagen hydrolysis and glycolysis. These anaerobic pathways rely on endogenous fuels, and the abundance of phosphagen kinases and glycolytic enzymes that are present throughout the sarcoplasm make diffusion distances very short. However, diffusion limitation of aerobic metabolism, which depends on the movement of oxygen from the blood to the mitochondria, could affect the rate of post-contractile recovery and therefore limit an animal's ability to undergo multiple high-force escape responses during predator–prey interactions (Kinsey et al., 2005; Nyack et al., 2007; Jimenez et al., 2008). Nevertheless, large increases in diffusion distances in muscle due to hypertrophic growth are prevalent among many animals including mammals, although the most extreme cases are found in anaerobic muscle fibers of crustaceans and fish species (Boyle et al., 2003; Johnson et al., 2004; Nyack et al., 2007; Jimenez et al., 2008). So, why might there be positive selection for large fiber sizes? Johnston and colleagues (Johnston et al., 2003; Johnston et al., 2004; Johnston et al., 2006) proposed the optimal fiber size hypothesis, which states that the large fibers in some fishes reflect selection to minimize maintenance costs, while balancing these cost savings against the need for small fibers that promote rapid diffusive flux. The American lobster is an ideal study organism to test this hypothesis because its abdominal musculature comprises 20–30% of the whole-animal body mass and it is activated only during escape responses. Hence, these animals have to maintain a large mass of muscle tissue that is only rarely used. Further, as the animal increases in size, it relies less on tail flipping to escape predators and more on defensive behaviors (Lang et al., 1977). Therefore, this muscle group may be under strong selective pressure to minimize metabolic costs associated with tissue maintenance.

The costs associated with the Na^+/K^+-ATPase in *H. americanus* was 40–50% of the muscle resting metabolic rate, which is consistent with previous studies in skeletal muscle from sheep (Gregg and Milligan, 1982), mice (Gregg and Milligan, 1980), rats (Asano et al., 1976) and calves (Gregg and Milligan, 1982), although Pörtner and colleagues (Pörtner et al., 2000) found that Na^+/K^+-ATPase costs were only 17–25% of basal metabolic costs in aerobic muscle tissue of the lugworm *Sipunculus nudus*. Both the cost and maximal activity of the Na^+/K^+-ATPase were 2-fold higher in smaller fibers present in juveniles than in the larger fibers of adults. This change in cost and activity during growth corresponds with the same fold-change in fiber SA:V, suggesting that pump density does not change during growth. Further, only the Na^+/K^+-ATPase experiments showed an interaction between size class and treatment on AP depletion rate (Fig. 4). That is, there was a significant size-dependent reduction in the AP depletion rate (compared with the basal rate) when the Na^+/K^+-ATPase was inhibited, but not when the SR Ca^{2+}-ATPase or transcription and translation were inhibited. These findings are consistent with expectations of the optimal fiber size hypothesis proposed by Johnston and colleagues (Johnston et al., 2003; Johnston et al., 2004; Johnston et al., 2006), and to our knowledge provide the first experimental evidence of the selective factors that may control minimal fiber size.

The AP depletion rate in the presence of nifidipine and thapsigargin, which allowed us to measure the cost of Ca^{2+} cycling, was 30–50% of the basal metabolic rate in small and large muscle fibers of *H. americanus*, respectively, and had nearly the same absolute cost in the two size classes, as expected (Fig. 4). Maximal Ca^{2+}-ATPase activity assays yielded values that were higher than reported values in the literature from rainbow trout and crucian carp heart, and also from plantaris in rats (Fig. 5B) (Aho and Vornanen, 1998; Inashima et al., 2003). However, maximal activity of Ca^{2+}-ATPase in crustacean muscle has been reported to be up to two orders of magnitude greater than that of comparable vertebrate Ca^{2+}-ATPases in muscle (Ahearn et al., 2004; Van der Kloot, 1969; Baskin, 1971) and the TEM images used for mitochondrial volume density in this study revealed large amounts of SR throughout the tissue compared with fish tissue (data not shown). Deamer (Deamer,

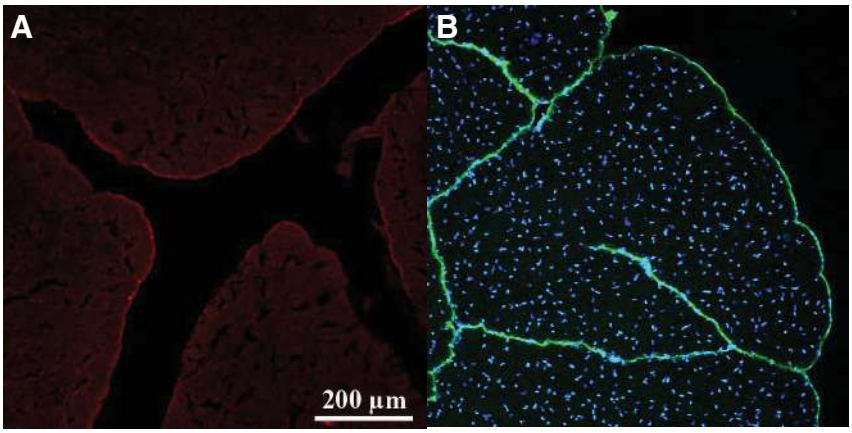

Fig. 6. (A) Examples of images collected using confocal microscopy at a magnification of 10×. Immunolocalization of the Na^+/K^+-ATPase revealed that Na^+/K^+-ATPase pumps were largely localized to the sarcolemma in adult *H. americanus* abdominal muscle fibers (*N*=3). (B) Cross-section of white abdominal muscle fibers from wheat germ agglutinin Alexa Fluor 488 (WGA)-injected adult lobsters. Green fluorescent WGA labeling delineates fiber sarcolemma as well as sarcolemmal clefts. Nuclei are labeled with the blue-fluorescent probe DAPI.

1973) suggested that the purified lobster Ca^{2+}-ATPase is very similar to that in mammals, although the specific activity of the enzyme was among the highest reported. The lack of a fiber size effect is again consistent with the optimal fiber size hypothesis, as the SR Ca^{2+}-ATPase is not associated with the sarcolemmal membrane.

Muscle fibers are a multi-nucleated syncytium, and in adult crustaceans myonuclei are uniformly distributed throughout the muscle fiber, which is different from the mammalian paradigm where myonuclei are usually at the fiber periphery and are associated with the sarcolemma (Bruusgaard et al., 2003; Hardy et al., 2009; Hardy et al., 2010; Jimenez et al., 2010) (Fig. 6B). However, calculated mean values of nuclear number volume (Fig. 5C) are similar to those found in blue crab, chicken, rat and human muscle (Allen et al., 1996; Ohira et al., 1999; Rosser et al., 2002; Hardy et al., 2009; Jimenez et al., 2010). The cost of protein turnover in these fibers was 14% and 11% of the muscle basal metabolic rate in juvenile and adult animals, respectively, although there was no significant interaction of size class and inhibitor treatment on the rate of AP depletion (Fig. 4). The nuclear number volume in these fibers was proportional to the cost of transcription+translation, although unlike the cost experiments the number volume was significantly higher in small fibers from juveniles than in large fibers from adults (Fig. 5C). It is possible that the greater investment in nuclei in juveniles than adults is related to higher growth rates in smaller animals. Nevertheless, these findings are not inconsistent with the optimal fiber size hypothesis as the nuclei are clearly independent of the fiber SA:V (Fig. 6B).

To assess the impact of fiber size on whole-animal metabolic rate, we estimated the percentage of $\dot{V}_{O_2}$ devoted to the Na^+/K^+-ATPase in muscle. Whole-animal $\dot{V}_{O_2}$ and Na^+/K^+-ATPase costs were directly compared by assuming a percentage of body mass that is abdominal muscle (22% for both size classes), 22.41 O_2 mol^{-1} O_2, an ATP:O_2 ratio of 6 and an intracellular water content that was 70% of wet mass. We used whole-animal $\dot{V}_{O_2}$ values for lobster from the literature (Bridges and Brand, 1980; Logan and Epifano, 1978), which we converted to 2.90 µmol ATP g^{-1} min^{-1} for juvenile lobsters and 0.33 µmol ATP g^{-1} min^{-1} for adult lobsters. Only 0.4% of whole-animal $\dot{V}_{O_2}$ is devoted to the maintenance of the membrane potential in abdominal muscle of juvenile lobsters, while 2.6% of $\dot{V}_{O_2}$ is devoted to this in adult lobsters. However, if we extrapolate the cost of the Na^+/K^+-ATPase to a smaller cell based on the SA:V relationship (Fig. 7), then for a muscle composed of fibers that are 40 µm in diameter (typical for many fiber types), the cost of membrane potential maintenance in abdominal muscle would be 48% of the total O_2 consumption in an adult lobster. This suggests a substantial metabolic advantage of the large fiber sizes found in the lobster.

The optimal fiber size hypothesis states that larger fibers are less costly to maintain, and therefore there is selective pressure for fibers to be as large as possible without incurring diffusion limitation. The present study provides evidence that large fibers are, in fact, cheaper to maintain, and most of the difference in resting metabolic rate of the abdominal fibers is due to differences in the Na^+/K^+-ATPase costs between juvenile and adult animals (Fig. 4B). The basis for this appears to be simple geometry, as both the Na^+/K^+-ATPase activity and cost were proportional to the fiber SA:V. However, while there appears to be selective pressure to make fibers large, they do not appear to be as large as they can be. Fig. 7 shows that for a $\dot{V}_{max}$ for aerobic ATPase function of 1.2 mmol l^{-1} ATP min^{-1}, which we believe is a reasonable upper rate for this tissue

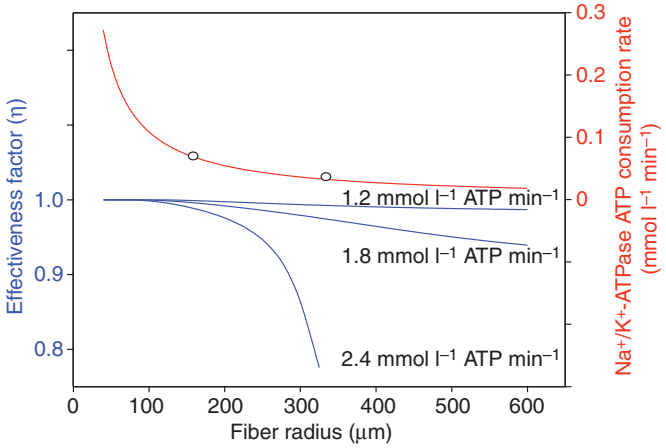

Fig. 7. Relationship between the Na^+/K^+-ATPase cost and diffusion limitation of aerobic metabolism during hypertrophic fiber growth in *H. americanus*. A curve (red line) that defines the SA:V of a cylindrical fiber (excluding the ends) was iteratively fitted to the experimental measurements (circles) of Na^+/K^+-ATPase cost. If the Na^+/K^+-ATPase pump density is constant, then this curve can be used to predict the Na^+/K^+-ATPase cost over a broader growth range than was available in our two size classes. Blue lines represent mathematical calculations of the effectiveness factor (η), which is an index of diffusion limitation, for aerobic metabolism at several $\dot{V}_{max}$ values of aerobic ATP consumption. At an aerobic ATP consumption $\dot{V}_{max}$ of 1.2 mmol l^{-1} ATP min^{-1}, which is likely the most reasonable for this tissue, aerobic metabolism is not substantially limited by diffusion (indicated by a value for η at or near 1). See Results for additional details.

based on mitochondrial volume density and previous work (Kinsey et al., 2005; Jimenez et al., 2008), fibers could grow to considerably larger sizes and not reach diffusion limitation. This finding would seem to be at odds with the optimal fiber size hypothesis. However, Fig. 7 also shows that once fibers reach a radius of about 300 μm, there is very little reduction in SA:V as fibers continue to grow. Therefore, the selective pressure that drives fibers to be large may be gradually relieved as they attain large sizes. In contrast, there is a very large change in SA:V in smaller fibers, and the selective pressure may be much greater in the early stages of animal growth (in animals smaller than we could acquire). This also suggests that the optimal fiber size hypothesis proposed by Johnston and colleagues (Johnston et al., 2003; Johnston et al., 2004; Johnston et al., 2006) to explain the very large fibers in some fish may actually be most applicable to muscle with fibers that do not grow to such extraordinary sizes, including that in mammals. Thus, the present study provides support for the hypothesis that muscle fiber minimal size is governed, at least in part, by the reduced maintenance costs afforded by large fibers.

ACKNOWLEDGEMENTS

We would like to thank Dr Sonya Pyott for her guidance in immunohistochemistry procedures; Dr Bob Roer for his help with Na^+/K^+-ATPase activity assays; Dr Dick Dillaman and Mr Mark Gay for their help with microscopy techniques; Beth Basinski and Bob Glenn from Massachusetts Division of Marine Fisheries and Anita Metzler from the New England Aquarium lobster lab for providing us with juvenile *H. americanus*. The α5 antibody, mouse anti-chicken IgG, was obtained from Developmental Studies Hybridoma Bank and was developed by Dr M. Fambrough.

FUNDING

This research was supported by the National Science Foundation [IOS-0316909 and IOS-0719123 to S.T.K., IOS-0315883 and IOS-0718499 to B.R.L.].

REFERENCES

Ahearn, G. A., Mandal, P. K. and Mandal, A. (2004). Calcium regulation in crustaceans during the molt cycle: a review and update. *Comp. Biochem. Physiol.* **137A**, 247-257.

Aho, E. and Vornanen, M. (1998). Ca^{2+}-ATPase activity and Ca^{2+} uptake by sarcoplasmic reticulum in fish heart: effects of thermal acclimation. *J. Exp. Biol.* **201**, 525-532.

Allen, D. L., Linderman, J. K., Roy, R. R., Bigbee, A. J., Grindeland, R. E., Mukku, V. and Edgerton, V. R. (1996). Myonuclear number and myosin heavy chain expression in rat soleus single muscle fibers after spaceflight. *J. Appl. Physiol.* **81**, 145-151.

Asano, Y., Liberman, U. A. and Eldelman, I. S. (1976). Relationships between Na^+-dependent respiration and Na^+K^+-adenosine triphosphatase activity in rate skeletal muscle. *J. Clin. Invest.* **57**, 368-376.

Barr, D. J., Green, H. J., Lounsbury, D. S., Rush, J. W. E. and Ouyang, J. (2005). Na^+-K^+-ATPase properties in rat heart and skeletal muscle 3 mo after coronary artery ligation. *J. Appl. Physiol.* **99**, 656-664.

Barradas, C., Wilson, J. M. and Dunel-Erb, S. (1999). Na^+/K^+-ATPase activity and immunocytochemical labeling in podobranchial filament and lamina of the freshwater crayfish *Astacus leptodactylus* Eschscholtz: evidence for the existence of sodium transport in the filaments. *Tissue Cell* **31**, 523-528.

Baskin, R. J. (1971). Ultrastructure and calcium transport in crustacean muscle microsomes. *J. Cell Biol.* **48**, 49-60.

Beard, D. A. (2005). A biophysical model of the mitochondrial respiratory system and oxidative phosphorylation. *PloS Comput. Biol.* **2**, 8.

Bittner, G. D. and Traut, D. L. (1978). Growth of crustacean muscles and muscle fibers. *J. Comp. Physiol.* **124**, 277-285.

Boyle, K. M., Dillaman, R. M. and Kinsey, S. T. (2003). Mitochondrial distribution and glycogen dynamics suggest diffusion constraints in muscle fibers of the blue crab, *Callinectes sapidus*. *J. Exp. Zool.* **297A**, 1-16.

Bridges, C. R. and Brand, A. R. (1980). Oxygen consumption and oxygen-independence in marine crustaceans. *Mar. Ecol. Prog. Ser.* **2**, 133-141.

Bruusgaard, J. C., Liestøl, K., Ekmark, M., Kollstad, K. and Gunderson, K. (2003). Number and spatial distribution of nuclei in the muscle fibers of normal mice studies *in vivo*. *J. Physiol.* **551**, 467-478.

Burpee, J. L. E. L., Bardsley, R. M., Dillaman, W. O., Watanabe, W. O. and Kinsey, S. T. (2010). Scaling with body mass of mitochondrial respiration from the white muscle of three phylogenetically, morphologically, and behaviorally disparate teleost fishes. *J. Comp. Physiol. B* **180**, 967-977.

Carroll, S., Nicotera, P. and Pette, D. (1999). Calcium transients in single fibers of low-frequency stimulates fast-twitch muscle of rat. *Am. J. Physiol.* **277**, C1122-C1129.

Clausen, T., Everts, M. E. and Van Hardeveld, C. (1991). Significance of cation transport in control of energy metabolism and thermogenesis. *Physiol. Rev.* **71**, 733-774.

Combs, C. A. and Ellington, W. R. (1995). Graded intracellular acidosis produces extensive and reversible reductions in the effective free energy change of ATP hydrolysis in a molluscan muscle. *J. Comp. Physiol. B* **165**, 203-212.

Dasika, S. K., Kinsey, S. T. and Locke, B. R. (2011). Oxygen and high energy phosphate diffusional constraints on energy metabolism in skeletal muscle. *Biotechnol. Bioeng.* **108**, 104-115.

Deamer, D. W. (1973). Isolation and characterization of a lysolecithin-adenosine triphosphatase complex from lobster microsomes. *J. Biol. Chem.* **15**, 5477-5485.

Fine, M. L., Bernard, B. and Harris, T. M. (1993). Functional morphology of toadfish sonic muscle fibers: relationship of possible fiber division. *Can. J. Zool.* **71**, 2262-2274.

Fraser, S. F. and McKenna, M. J. (1998). Measurement of Na^+,K^+-ATPase activity in human skeletal muscle. *Anal. Biochem.* **258**, 63-67.

Gill, M., France, J., Summers, M., McBride, B. W. and Milligan, L. P. (1989). Simulation of energy costs associated with protein turnover and Na^+-K^+-transport in growing lambs. *J. Nutr.* **119**, 1287-1299.

Gregg, V. A. and Milligan, L. P. (1980). Inhibition by ouabain of the O_2 consumption of the mouse (*Mus musculus*) soleus and diaphragm muscles. *Gen. Pharmacol.* **11**, 323-325.

Gregg, V. A. and Milligan, L. P. (1982). *In vitro* energy costs of Na^+-K^+-ATPase activity and protein synthesis in muscle from calves differing in age and breed. *Br. J. Nutr.* **48**, 65-71.

Györke, S. and Palade, P. (1992). Calcium-induces calcium release in crayfish skeletal muscle. *J. Physiol.* **457**, 195-210.

Hardy, K. M., Dillaman, R. M., Locke, B. R. and Kinsey, S. T. (2009). A skeletal muscle model of extreme hypertrophic growth reveals the influence of diffusion on cellular design. *Am. J. Physiol.* **296**, R1855-R1867.

Hardy, K. M., Lema, S. C. and Kinsey, S. T. (2010). The metabolic demands of swimming behavior influence the evolution of skeletal muscle fiber design in the brachyuran crab family *Portunidae*. *Mar. Biol.* **157**, 221-236.

Howard, C. V. and Reed, M. G. (1998). *Unbiased Stereology, 3-Dimensional Measurements in Microscopy*. Oxford, UK: BIOS, Scientific.

Inashima, S., Matsunaga, S., Yasuda, T. and Wada, M. (2003). Effect of endurance training and acute exercise on sarcoplasmic reticulum function in rat fast- and slow-twitch skeletal muscles. *Eur. J. Appl Physiol.* **89**, 142-149.

Jimenez, A. G. J., Locke, B. R. and Kinsey, S. T. (2008). The influence of oxygen and high-energy phosphate diffusion on metabolic scaling in three species of tail-flipping crustaceans. *J. Exp. Biol.* **211**, 3214-3225.

Jimenez, A. G. J., Kinsey, S. T., Dillaman, R. M. and Kapraun, D. F. (2010). Nuclear DNA content variation associated with muscle fiber hypertrophic growth in decapod crustaceans. *Genome* **53**, 161-171.

Jobling, M. (1994). *Fish Bioenergetics*. London: Chapman and Hall.

Johnson, L. K., Dillaman, R. M., Gay, D. M., Blum, J. E. and Kinsey, S. T. (2004). Metabolic influences of fiber size in aerobic and anaerobic locomotor muscles of the blue crab, *Callinectes sapidus*. *J. Exp. Biol.* **207**, 4045-4056.

Johnston, I. A., Fernandez, D., Calvo, J., Vieira, V. L. A., North, T. W., Abercromby, M. and Garland, T., Jr (2003). Reduction in muscle fibre number during the adaptive radiation of Notothenioid fishes: a phylogenetic perspective. *J. Exp. Biol.* **206**, 2595-2609.

Johnston, I. A., Abercromby, M., Vieria, V. L. A., Sigursteindottir, R. J., Kristjansson, B. K., Sibthorpe, D. and Skulason, S. (2004). Rapid evolution of muscle fibre number in post-glacial populations of charr *Salvelinus alpinus*. *J. Exp. Biol.* **207**, 4343-4360.

Johnston, I. A., Abercromby, M. and Andersen, O. (2006). Muscle fibre varies with haemoglobin phenotype on Atlantic cod as predicted by the optimal fibre number hypothesis. *Biol. Lett.* **2**, 590-592.

Kinsey, S. T. and Ellington, W. R. (1996). ^1H- and ^{31}P-Nuclear magnetic resonance studies of L-lactate transport in isolated muscle fibers from the spiny lobster, *Panulirus argus*. *J. Exp. Biol.* **199**, 2225-2234.

Kinsey, S. T., Pathi, P., Hardy, K. M., Jordan, A. and Locke, B. R. (2005). Does intracellular metabolite diffusion limit post-contractile recovery in burst locomotor muscle? *J. Exp. Biol.* **208**, 2641-2652.

Kinsey, S. T., Hardy, K. M. and Locke, B. R. (2007). The long and winding road: influences of intracellular metabolite diffusion on cellular organization and metabolism in skeletal muscle. *J. Exp. Biol.* **210**, 3505-3512.

Kinsey, S. T., Locke, B. R. and Dillaman, R. M. (2011). Molecules in motion: influences of diffusion on metabolic structure and function in skeletal muscle. *J. Exp. Biol.* **214**, 263-274.

Lang, F., Govind, C. K., Costello, W. J. and Greene, S. I. (1977). Developmental neuroethology: changes in escape and defensive behavior during growth of the lobster. *Science* **197**, 682-685.

Logan, D. T. and Epifano, C. E. (1978). A laboratory energy balance for the larvae and juveniles of the American lobster *Homarus americanus*. *Mar. Biol.* **47**, 381-389.

Lowry, O. H. and Passonneau, J. V. (1972). Lactate: Method II. In *A Flexible System of Enzymatic Analysis*. New York, London: Academic Press.

Milligan, L. P. and McBride, B. W. (1985). Energy costs of ion pumping by animal tissues. *J. Nutr.* **115**, 1374-1382.

Nyack, A. C., Locke, B. R., Valencia, A., Dillaman, R. M. and Kinsey, S. T. (2007). Scaling of post-contractile phosphocreatine recovery in fish white muscle: effect of intracellular diffusion. *Am. J. Physiol.* **292**, R1-R12.

Ohira, Y., Yoshinaga, T., Ohara, M., Nonaka, I., Yoshioka, K. T., Shenkman, B. S., Kozlovskaya, I. B., Roy, R. R. and Edgerton, V. R. (1999). Myonuclear domain and myosin phenotype in human soleus after bed rest with or without loading. *J. Appl. Physiol.* **87**, 1776-1785.

Peachey, L. D. (1967). Membrane systems of crab fibers. *Am. Zool.* **7**, 505-513.

Pörtner, H. O., Bock, C. and Reipschlager, A. (2000). Modulation of the cost of pH_i regulation during metabolic depression: A ^{31}P-NMR study in invertebrate (*Sipunculus nudus*) isolated muscle. *J. Exp. Biol.* **203**, 2417-2428.

Priester, C., Morton, L. C., Kinsey, S. T., Watanabe, W. O. and Dillaman, R. M. (2011). Growth patterns and nuclear distribution in white muscle fibers from black sea bass *Centropristis striata* (Linnaeus): evidence for the influence of diffusion. *J. Exp. Biol.* **214**, 1230-1239.

Rolfe, D. F. S. and Brand, M. D. (1996). Contribution of mitochondrial proton leak to skeletal muscle respiration and to standard metabolic rate. *Am. J. Physiol.* **271**, C1380-C1389.

Rolfe, D. F. S. and Brown, G. C. (1997). Cellular energy utilization and molecular origin of standard metabolic rate in mammals. *Physiol. Rev.* **77**, 731-758.

Rosser, B. W. C., Dean, M. S. and Bandman, E. (2002). Myonuclear domain size varies along the lengths of maturing skeletal muscle fibers. *Int. J. Dev. Biol.* **46**, 747-754.

Rosser, K. L. and Sherman, R. G. (1978). Invaginated membrane in crustacean tonic muscle fibers: estimated of membrane capacitance. *Am. J. Physiol.* **235**, C220-C226.

Sandiford, S. D. E., Green, H. J. and Ouyang, J. (2005). Mechanisms underlying increases in rat soleus Na^+-K^+-ATPase activity by induced contractions. *J. Appl. Physiol.* **99**, 2222-2232.

Schmalbruch, H. and Hellhammer, U. (1977). The number of nuclei in adult rat muscles with special reference to satellite cells. *Anat. Rec.* **189**, 169-175.

Selverston, A. (1967). Structure and function of transverse tubular system in crustacean muscle fibers. *Am. Zool.* **7**, 515-525.

Simonides, W. S. and van Hardeveld, C. (1990). An assay for sarcoplasmic reticulum Ca^{2+}-ATPase activity in muscle homogenates. *Anal. Biochem.* **191**, 321-331.

Smith, E. and Morrison J. F. (1969). Kinetic studies on the arginine kinase reaction. *J. Biol. Chem.* **244**, 4224-4234.

Swaminathan, R., Chan, E. L. P., Sin, L. Y., King, N. S., Fun, N. S. and Chan, A. Y. S. (1989). The effect of ouabain on metabolic rate in guinea pigs: estimation of energy cost of sodium pump activity. *Br. J. Nutr.* **61**, 467-473.

Valente, L. M. P., Rocha, E., Gomes, E. F. S., Silva, M. W., Oliveira, M. H., Monteiro, R. A. F. and Fauconneau, B. (1999). Growth dynamics of white and red muscle fibers in fast- and slow-growing strains of rainbow trout. *J. Fish Biol.* **55**, 675-691.

Van der Kloot, W. (1969). Calcium uptake by isolated sarcoplasmic reticulum treated with dithiothreitol. *Science* **164**, 1294-1295.

Van Wessel, T., de Haan, A., van der Laarse, W. J. and Jaspers, R. T. (2010). The muscle fiber type-fiber size paradox: hypertrophy or oxidative metabolism. *Eur. J. Appl. Physiol.* **110**, 665-694.

Weatherley, A. and Gill, H. (1987). *Biology of Fish Growth*. San Diego, CA: Academic Press.

Wright, C. S. (1984). Structural comparison of the two distinct sugar binding sites in wheat germ agglutinin isolectin II. *J. Mol. Biol.* **178**, 91-104.

Zurlo, F., Larson, K., Bogardus, C. and Ravussin, E. (1990). Skeletal muscle metabolism is a major determinant of resting energy expenditure. *J. Clin. Invest.* **86**, 1423-1427.